Journal of Magnetic Resonance **151,** 228–234 (2001)
doi:10.1006/jmre.2001.2366, available online at http://www.idealibrary.com on IDEAL®

Circularly Polarized RF Magnetic Fields for Spin-1 NQR

J. B. Miller,*,[1] B. H. Suits,† and A. N. Garroway*

*Chemistry Division, Code 6120, Naval Research Laboratory, Washington, DC 20375-5342; and †Physics Department, Michigan Technological University, Houghton, Michigan 49931-1295

E-mail: joel.b.miller@nrl.navy.mil

Received June 26, 2000; revised April 20, 2001; published online July 3, 2001

The low sensitivity of nuclear quadrupole resonance (NQR) of powders is due, in part, to the inability to efficiently excite and detect nuclei at all crystal orientations. Here we describe the use of circularly polarized RF magnetic fields for excitation followed by detection of the resultant circular RF magnetization in $I = 1$ NQR to increase the fraction of nuclei excited and detected. We show that the technique can greatly improve the effective RF field homogeneity and increase the largest signal amplitude by a factor of 1.72. In favorable cases, the resulting circularly polarized NQR signal can be separated from linearly polarized magnetoacoustic and piezoelectric ringing artifacts that occur in some NQR materials detection applications.

Key Words: **NQR; signal-to-noise, spin 1; rotating field; circularly polarized.**

INTRODUCTION

NQR is frequently referred to as "NMR at zero field," the nuclear levels being split by internal electric field gradients rather than an externally applied magnetic field. For the case of nuclei with spin $I = 1$ there will be, in general, three allowed transition frequencies (*1*), assuming $\eta \neq 0$. Much understanding can be gained by treating the individual transitions as those of isolated $I = \frac{1}{2}$ nuclei in a high magnetic field, the so-called "effective spin-$\frac{1}{2}$ model" (*2, 3*). The analogy is good for the case of single-crystal NQR, but certain precautions must be taken when considering powders. Unlike NMR, where the quantization axis is imposed by the experimenter via the applied static magnetic field and has a well-defined direction in the laboratory reference frame, in NQR a quantization axis for each nucleus is determined by the charge distribution about the nucleus and is tied to a molecular reference frame. Specifically, the NQR quantization axis is determined by the quadrupole principle axis system (QPAS) defined by the electric field gradient tensor as seen by that nucleus. For nuclear spin $I = 1$, each of the three possible transitions is associated with one of the three orthogonal axes of the QPAS (*1*). In a powder, there is no unique direction in the laboratory defining the quantization axis of the sample. Moreover, the nutation rate induced by the applied RF field, B_1, used to excite the nuclei, depends on the projection of that RF field on the QPAS axis associated with the transition being excited, leading to a broad distribution of nutation rates throughout a powder sample. In addition, the detection efficiency also depends on the projection of the RF field (of the receiver coil) on the same QPAS axis.

Clearly there exists a significant portion of the sample that is only weakly excited by the RF magnetic field and hence will provide a reduced signal after an RF pulse. However even this weak excitation is enough to saturate these spins when, for example, multiple-pulse sequences are used to increase the signal-to-noise ratio (SNR) (*4*). Therefore moving the sample or the coil and repeating the experiment to excite and detect some of these spins is generally not advantageous. Here we propose to improve the sensitivity of NQR measurements using a circularly polarized RF field, i.e., an RF field rotating on the timescale of the NQR resonance frequency, to detect a larger fraction of the crystallites in our powder sample. We refer to the technique as "circularly polarized NQR."

RESPONSE TO A CIRCULARLY POLARIZED FIELD

To understand the advantages of circularly polarized NQR we must compare the effects of linearly polarized and circularly polarized RF fields in NQR and NMR. A linearly polarized RF magnetic field always has its direction along a fixed axis in the laboratory frame. For example a linearly polarized RF magnetic field along the z axis is given by

$$\mathbf{B}_{1\mathrm{L}} = B_1 \cos(\omega t)\mathbf{z}. \qquad [1]$$

A circularly polarized RF magnetic field has constant amplitude, but rotates in the laboratory reference frame. It is the sum of two spatially orthogonal, linearly polarized fields 90° out of phase. For example a circularly polarized RF magnetic field in the x–y plane is given by

$$\mathbf{B}_{1\mathrm{C}} = B_1(\cos \omega t\mathbf{x} + \sin \omega t\mathbf{y}). \qquad [2]$$

We note that a linearly polarized field can be written as the sum

[1] To whom correspondence should be sent. Fax: (202) 767-0594.

1090-7807/01 $35.00

of two circularly polarized fields whose frequencies differ in sign. A coil that produces a linearly or circularly polarized RF field is referred to as a linearly or circularly polarized coil respectively. A circularly polarized coil is easily constructed from two orthogonal linearly polarized coils electrically connected 90° out of phase. For the sake of the discussion that follows, we will assume such an arrangement.

In NMR, after excitation, the spins precess about the static magnetic field, producing a circularly polarized RF field. The signal observed in a standard NMR experiment, i.e., from a linearly polarized receiver coil, is proportional to the time derivative of the projection of the time-dependent magnetic field from the spins on the coil axis. Such a linearly polarized coil cannot differentiate signals, or noise, at the Larmor frequency, ω_0, from signals at $-\omega_0$. In the rotating frame we commonly use quadrature detection to differentiate frequencies at $\omega_0 + \delta$ from $\omega_0 - \delta$ and obtain a $2^{\frac{1}{2}}$ increase in SNR by separating the noise contributions at the two frequencies. Hoult *et al.* (*5, 6*) showed that laboratory frame quadrature detection, i.e., detection with a circularly polarized coil, differentiates signals at ω_0 from signals at $-\omega_0$, resulting in an additional $2^{\frac{1}{2}}$ increase in SNR. Put another way, a circularly polarized coil detects the spins along two orthogonal axes, doubling the measured signal, and under the assumption that the noise currents detected along the two axes are independent, the SNR is increased by $2^{\frac{1}{2}}$. Note that for NMR we have not required the spins to be irradiated with a circularly polarized field to obtain the enhanced SNR with circularly polarized detection.

In NMR, the effective B_1 field strength per unit input power is increased by $2^{\frac{1}{2}}$ with a circularly polarized transmitter coil because a linearly polarized coil uses half the available power to create the (useless) counterrotating circularly polarized RF field. (We assume that each of the component coils of the circularly polarized coil is as efficient as the linearly polarized coil.) Below we show that the use of circularly polarized fields in NQR results in more efficient use of RF power and an increase in SNR, *but for entirely different reasons*.

Unlike NMR, where nuclear precession about B_0 creates a circularly polarized RF field, in NQR the nuclear magnetization *oscillates* along the QPAS axis, creating a linearly polarized RF field. To understand why circularly polarized excitation fields and detection coils are useful in NQR, we must consider the effects of the distribution of crystallite orientations in a powder on B_1 efficiency and SNR. For an $I = 1$ nucleus with a QPAS component along (θ, φ), transitions between levels associated with this QPAS component can be induced by irradiating along (θ, φ). In a standard pulsed NQR experiment, we use a linearly polarized coil for both excitation and detection. In Fig. 1, such a situation is depicted using a coil at $\theta = 0$ (the z coil), in a spherical coordinate frame, resulting in the RF field described by Eq. [1]. The exciting field seen by the nucleus is the projection of $\mathbf{B}_{1\mathrm{L}}$ onto the QPAS axis:

$$\mathbf{B}_{1\mathrm{L}}(\theta, \varphi) = B_{1\mathrm{L}} \cos\theta, \qquad [3]$$

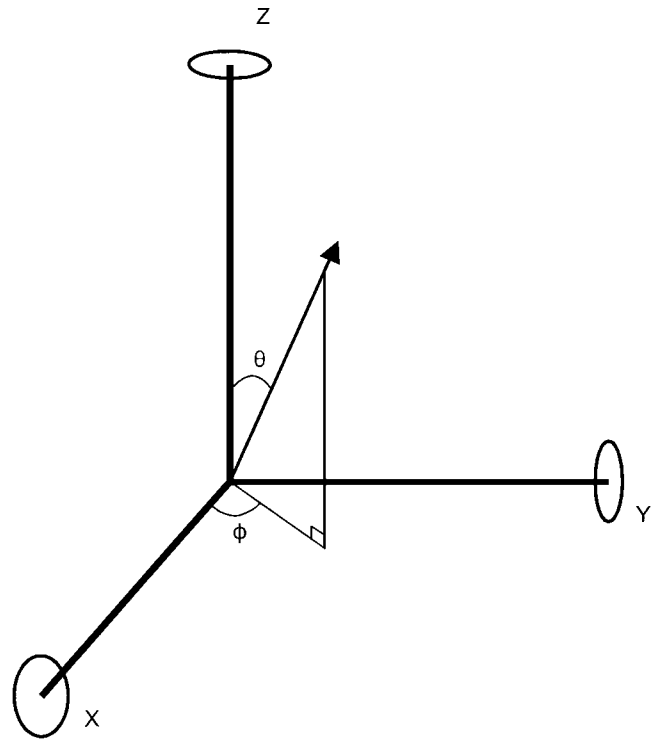

FIG. 1. Reference frame for x-, y-, and z-coil placement and showing the QPAS orientation along θ and φ in the laboratory frame.

The detected signal depends on the number of spins excited and the sensitivity of the coil to the evolving magnetization. The total signal amplitude detected is given by

$$S = \frac{1}{4\pi} \int_0^{2\pi} d\varphi \int_0^{\pi} d\theta \sin\left(\gamma B_{\mathrm{eff}}^{\mathrm{t}} \tau\right) B_{\mathrm{eff}}^{\mathrm{r}} \sin\theta, \qquad [4]$$

where $B_{\mathrm{eff}}^{\mathrm{r}}$ is the effective field of the receiving coil and $B_{\mathrm{eff}}^{\mathrm{t}}$ is the effective field of the transmitting coil. Using our linear z coil for both transmission and reception, we have $B_{\mathrm{eff}}^{\mathrm{r}} = \cos\theta$, and $B_{\mathrm{eff}}^{\mathrm{t}} = \mathbf{B}_{1\mathrm{L}}(\theta, \varphi)$. Substituting into Eq. [4] leads to the well-known result (*7*) that, in NQR of spin $I = 1$ powders, the variation of signal amplitude, S, following an RF pulse of length τ is given by

$$S_{\mathrm{L}} = \sqrt{\frac{\pi}{2\alpha}} J_{3/2}(\alpha), \qquad [5]$$

where $\alpha = \gamma B_1 \tau$ is the pulse nutation angle and $J_{3/2}$ is the Bessel function of order $\frac{3}{2}$. The maximum signal occurs at a nutation angle of 119° and accounts for only 43% of the potential signal that could be observed for an aligned single crystal. Equation [5] is plotted in Fig. 2 along with $\sin\alpha$, the variation in signal amplitude with α for NMR or single-crystal NQR.

To create a circularly polarized field, we need to generate two spatially orthogonal RF fields that are also 90° out of phase.

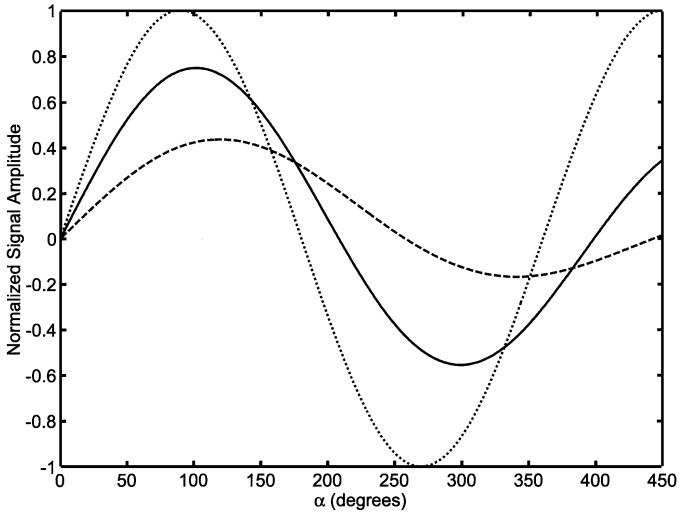

FIG. 2. Signal amplitude as a function of pulse nutation angle: $\sin\alpha$ for NMR (dotted line); Eq. [5] for linearly polarized NQR powder (dashed line); for circularly polarized NQR powder (solid line), twice the value of Eq. [8] is used to reflect to total signal available.

In Fig. 1, such a situation is depicted using two coils in the $\theta = \pi/2$ plane, at $\varphi = 0$ (the x coil) and $\varphi = \pi/2$ (the y coil), as described above. The resultant circularly polarized RF field (Eq. [2]) rotates in φ, at frequency ω. The projection of $\mathbf{B}_{1C}$ produced along (θ, φ) is

$$\mathbf{B}_{1C}(\theta, \varphi) = B_1 \cos(\omega t - \varphi)\sin\theta. \qquad [6]$$

Equation [6] describes a linearly polarized field phase-shifted by $-\varphi$ and scaled by $\sin\theta$. *Note that even though we apply a circularly polarized field, the effective field seen by each nucleus is linearly polarized*. Thus, $B_{\text{eff}}^{\text{t}} = B_1 \sin\theta$; however we chose to treat the signal detection with each coil separately: $B_{\text{eff}}^{\text{r}}(x) = \sin\theta\cos^2\varphi$; $B_{\text{eff}}^{\text{r}}(y) = \sin\theta\sin^2\varphi$. Using these values of $B_{\text{eff}}^{\text{r}}$ and $B_{\text{eff}}^{\text{t}}$ in Eq. [4] results in an integral for which no simple closed from solution has been found. (This integral is the same as that encountered by Bloom *et al*. (*8*) for a single-pulse, linearly polarized field, $I = \frac{3}{2}$ NQR with $\eta = 0$.) A tractable series solution is found using the relation

$$\sin(\alpha\sin\theta) = 2\sum_{k=0}^{\infty} J_{2k+1}(\alpha)\sin[(2k+1)\theta], \qquad [7]$$

resulting in

$$S_{\text{C}} = 2\left[\frac{J_1(\alpha)}{3} - \sum_{k=1}^{\infty}\frac{J_{2k+1}(\alpha)}{(2k+3)(2k+1)(2k-1)}\right]. \qquad [8]$$

The J_{2k+1} are Bessel functions of order $2k+1$ and α is the pulse nutation angle. This sum converges quickly, and results accurate to within 1% are obtained, keeping only the first two terms in the sum. As seen in Fig. 2, the sum of the peak signals from the two coils gives 74% of the optimally detected single crystal signal and 1.72 times the signal obtained with single-coil excitation and detection, at a pulse nutation angle of 102°. Assuming the received noise in the two coils is uncorrelated, this represents an increase in signal-to-noise ratio (SNR) of 21%. Note that for small flip-angle pulses as might be used for stochastic excitation (*9*), the signal gain approaches 2 with circular polarization, and the SNR gain approaches 41%.

Although the underlying physics is very different for the two cases, the use of circularly polarized excitation and detection similarly enhances B_1 efficiency and SNR in NMR and NQR. In the NMR case, we are using circularly polarized fields to excite and detect a circularly polarized magnetization. The circularly polarized field affects all the spins in the same way. The NMR spin system is inherently circularly polarized with only one sense of rotation: circularly polarized excitation improves excitation efficiency and circularly polarized detection increases SNR, independently of each other.

In the NQR case, most of the gain in SNR comes from more effectively exciting and detecting spins that otherwise are only weakly excited and detected with a linearly polarized coil. There is no SNR gain without circularly polarized excitation; in fact the SNR is reduced for the case of circularly polarized excitation and *linearly* polarized detection. Keep in mind that, unlike the NMR case, the NQR signal arises from an oscillating magnetization; therefore only a phase-shifted linearly polarized component of the rotating field excites the spins. The RF phases of spins with different orientations, each of which provides a linearly polarized contribution to the total signal, are choreographed by the circularly polarized field to result in a circularly polarized total magnetization. The sense of rotation is determined entirely by the sense of rotation of the applied RF field. The effective increase in B_1 is not a real increase: from Eqs. [1] and [2] we see that the maximum magnitude of $\mathbf{B}_{1C}$ is equal to the maximum magnitude of $\mathbf{B}_{1L}$, assuming that each of the component coils of the circularly polarized coil produces the same B_1 per unit input power ($B_1 \propto P^{\frac{1}{2}}$) as the linearly polarized coil. Rather, the circularly polarized field has a larger projection on the appropriate QPAS axis when averaged over all crystallite orientations. This is illustrated in Fig. 3 where we plot the distribution of normalized B_{eff} in a powder induced by a RF pulse of magnitude B_1, assuming a perfectly homogeneous coil. For the linearly polarized field case we see that all B_{eff} are equally probable, cf. Eq. [3]. In a circularly polarized field, the probability is strongly peaked at the maximum B_{eff}. The powder distribution of QPAS orientations effectively creates an inhomogeneous RF field. Circularly polarized excitation effectively homogenizes the RF field, resulting in the decrease in the pulse nutation angle necessary for the largest signal, and indirectly in the increase in SNR.

Hoult and coworkers (*5*, *6*) point out that coupling between the two orthogonal coils in a circularly polarized coil can lead to degradation of the coil quality factor, Q, potentially

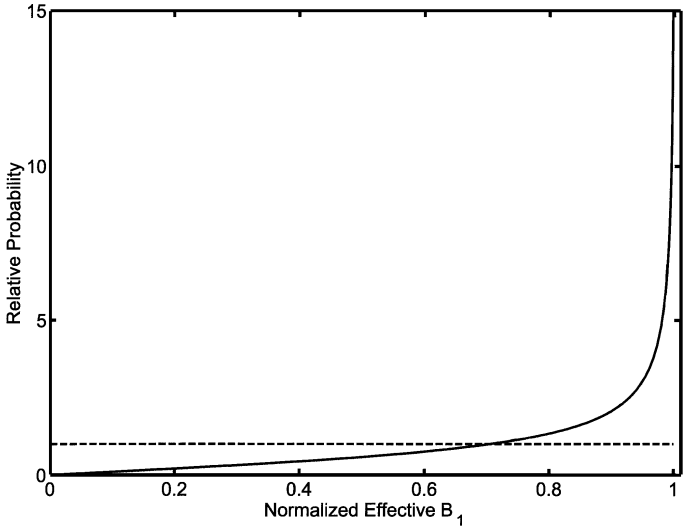

FIG. 3. Distribution of B_{eff} induced by a RF pulse of magnitude B_1, plotted as the probability of a given B_{eff} as a function of the normalized B_{eff}, B_{eff}/B_1. The solid line is the circularly polarized field, and the dashed line is the linearly polarized field for NQR. For a perfectly homogeneous RF coil, the NMR case is a delta function at $B_{\text{eff}}/B_1 = 1$.

nullifying the SNR gain. In NMR imaging, where circularly polarized excitation and detection are primarily used, sample noise usually dominates the coil noise; hence variations in Q have little effect on the overall SNR. In low-frequency and wide-line experiments we must be concerned with probe recovery time and bandwidth. In low-frequency NQR it is not uncommon for the signal linewidth to be a significant fraction of the probe bandwidth, or equivalently, T_2^* to be a fraction of the probe recovery time. Coupled with the commonly large variations of resonance frequency with temperature, the narrow bandwidths and long recovery times of high-Q probes can be serious problems. In such situations, circularly polarized excitation/detection will provide additional SNR advantages.

The total transmitter power required for an excitation pulse is another issue. In NQR, a 102° circularly polarized pulse requires approximately 50% more input power than a 119° linearly polarized pulse with coils of equal efficiency and equal pulse lengths. If the Q of the circularly polarized coil is lower than the linearly polarized coil, additional transmitter power is required. In many cases the available power is not the issue; rather electrical arcing in the probe limits the power that can be applied to the probe. Even though a circularly polarized coil requires 50% more power than an equally efficient linearly polarized coil, the peak voltage in the circularly polarized coil is 14% less than in the linearly polarized coil. This is a relatively modest advantage; in similar circumstances in NMR the peak voltage would be reduced by 30% for a circularly polarized coil.

We note that the idea of using circularly polarized fields for exciting and detecting $I = \frac{3}{2}$ NQR has been discussed in the literature (*10–12*) for purposes other than SNR enhancement.

RESULTS

In Fig. 4 we plot the measured NQR signal amplitude as a function of pulse nutation angle for both linearly polarized and circularly polarized excitation/detection (experimental details are provided in the next section). The linearly polarized data were fitted to the theoretical curve, Eq. [5], using the amplitude and B_1 as the fitting parameters. The circularly polarized data, detected in one spatial direction only, were scaled using the amplitude and B_1 parameters determined with the linearly polarized data: *there are no additional adjustable parameters in the fit of the circularly polarized data to the theoretical curve.* The circular polarization results verify the predicted signal amplitude, and the decreased pulse nutation angle required for maximum signal. For large nutation angles, the slower decrease in signal amplitude with increasing pulse nutation angle when using circularly polarized excitation is an indication of the increased effective homogeneity of the RF field.

The increased effective homogeneity of the RF field obtained with circularly polarized excitation has benefits beyond increased SNR. For example, the distribution of pulse nutation angles resulting from the use of linearly polarized excitation in NQR makes inversion-recovery, and even to some extent saturation-recovery, T_1 experiments difficult. The distribution of nutation angles leads to a relatively small fraction of the spins that are actually inverted by the first pulse. This problem is largely overcome by using circularly polarized excitation. In Fig. 5 we plot signal amplitude as a function of pulse nutation angle for a pulse sequence consisting of a variable nutation angle pulse followed by a short delay and then an effective "90°" pulse (102° for a circularly polarized field and 119° for a

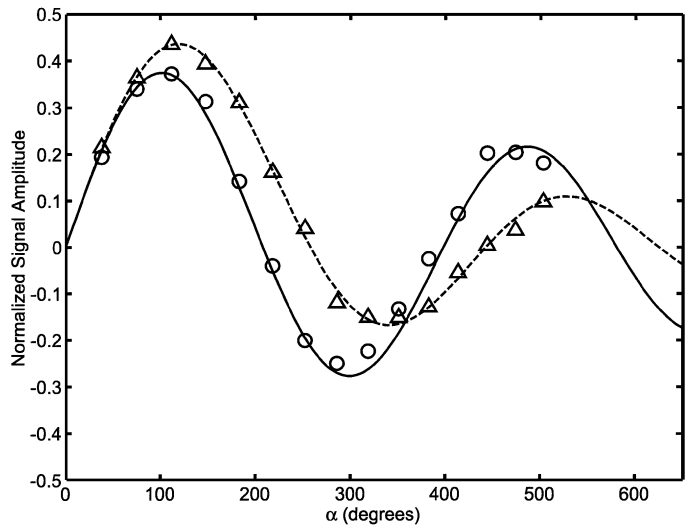

FIG. 4. Experimental and predicted signal amplitude as a function of pulse nutation angle: Eq. [5] for linearly polarized NQR powder (dashed line and open triangles for experimental data); Eq. [8] for circularly polarized field NQR powder (solid line and open circles for experimental data).

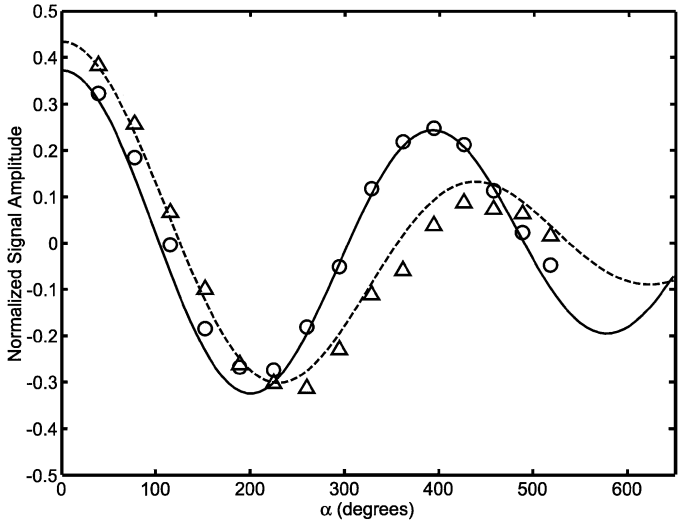

FIG. 5. Experimental and predicted signal amplitude as a function of pulse nutation angle for a two-pulse sequence: for linearly polarized NQR powder (dashed line and open triangles for experimental data); for circularly polarized field NQR powder (solid line and open circles for experimental data). The signal was recorded after excitation by a variable angle pulse, followed by a short delay (10 ms) and a pulse that produces maximum signal in an equilibrium system. The predicted signals were obtained by numerical integration as discussed in the text.

linearly polarized field). For circularly polarized excitation, very little magnetization is lost by inversion, particularly compared to linearly polarized excitation.

To realize the increased SNR with circularly polarized NQR, it is sufficient to appropriately phase-shift and sum the two quadrature components of the circularly polarized signal in the laboratory frame prior to detection by the receiver, effectively creating a linearly polarized signal. There are advantages to detecting the circularly polarized signal directly, however. Unlike NMR, where the sense of rotation about the static field is determined by the sign of the magnetogyric ratio, in NQR the sense of rotation is determined by the applied circularly polarized RF field (Fig. 6a). The phase of the NQR signal is determined by the phase of the RF pulse and any propagation delays in the receiver, just as in a standard NMR experiment. Potentially, this added information can be used to our advantage.

Low-frequency magnetic resonance experiments are often plagued by artifacts arising from magnetoacoustic ringing or piezoelectric ringing. This is especially true for measurements made for the purpose of *in situ* materials detection, where the environment surrounding the sample is often less than ideal. Like NQR signals, the ringing signals are inherently linearly polarized; however unlike NQR where there is a statistically large number of signal sources (the crystallites), there are usually only a few ringing sources that respond near the NQR frequency. There are rarely enough ringing sources to give a true "powder-averaged" signal; therefore the ringing artifacts generally do not give rise to perfectly circularly polarized signals. For a single ringing source, a linearly polarized signal is observed no matter what RF excitation is applied. The linearly polarized signal can be decomposed into two counterrotating circularly polarized signals of equal magnitude (Fig. 6b) that can be used to separate NQR and ringing signals. Not only is the phase of the ringing signal determined by the RF pulse phase and receiver propagation delays, like the NQR signal, but also by the source's orientation relative to the coils. This additional phase shift is clearly observed in Fig. 6b. If there is more than one ringing source at the same frequency, the resulting signal may be a combination of linearly and circularly polarized, i.e., elliptically polarized. In this case the two counterrotating circularly polarized signals are not the same (Fig. 6c) and the NQR and ringing signals cannot be completely separated. Nonetheless, some improvement will be observed.

EXPERIMENTAL

The use of crossed coils for circularly polarized NQR is complicated by the fact that, unlike NMR where the nuclei are sensitive only to two of the RF field components, in NQR all three components contribute to the excitation. In addition, two spatially orthogonal coils do not, in general, produce mutually orthogonal fields at all points in space. We have chosen to use a birdcage coil (*13, 14*) to partially circumvent this problem.

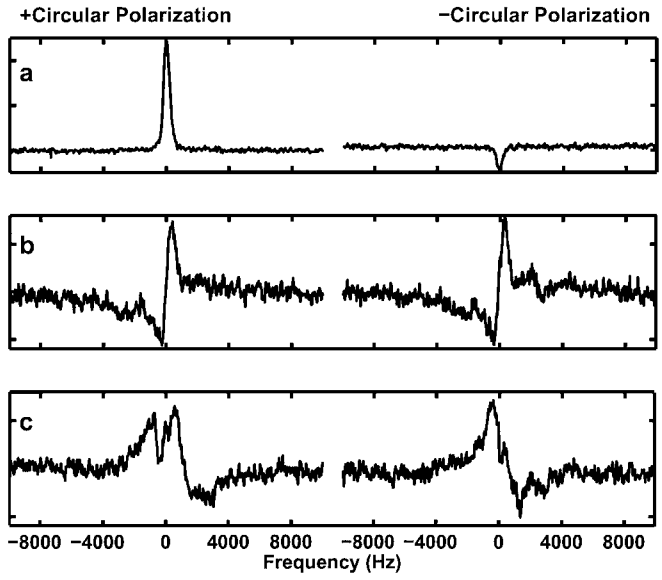

FIG. 6. Circularly polarized field data: (a) circularly polarized NQR signal from $NaNO_2$ at 4.6 MHz; (b) magnetoacoustic ringing signal, in the same frequency range, from a pair of locking pliers showing a linearly polarized signal (equal counterrotating circularly polarized signals); (c) magneto-acoustic ringing signal from the same pair of locking pliers after retensioning the lock spring, showing an elliptically polarized signal. The "+Circular Polarization" signals follow the applied circularly polarized field, and the "−Circular Polarization" signals rotate in the opposite sense. The circularly polarized signals were obtained in the rotating frame as described in the text. The same phase parameters were applied to all spectra.

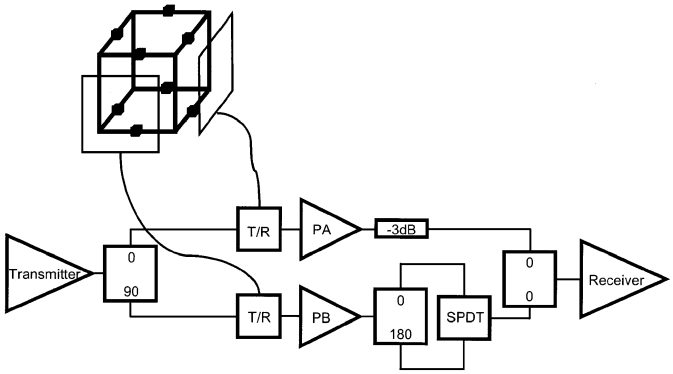

FIG. 7. Schematic of the circularly polarized NQR excitation/detection system. The components are identified in the text.

Two separate four-element birdcage coils were employed in this study. Our large volume birdcage coil (Fig. 7) is built as a cubic structure instead of the traditional cylindrical design. This design was originally chosen to allow the creation of RF fields in three orthogonal directions when the coil is tuned in a symmetric bandpass mode (*15*). For practical reasons, the experiments described here were performed with the coil tuned in highpass mode. The coil is constructed of $\frac{1}{2}$-in. copper pipe connected by brass fittings at the vertices, making a cube with 46 cm sides (100-L-enclosed volume). The coil is coarsely tuned with eight high-voltage mica capacitors and fine-tuned with ceramic capacitors and two variable capacitors. A small volume cylindrical birdcage coil (4.3 L) was constructed using 1-in. copper foil for the end rings and 0.039-in. copper ribbon wire for the rungs, and was tuned with ceramic chip capacitors and six vacuum variable capacitors. Both coils were matched by inductive coupling with two single-turn coils. The tuning and coupling are adjusted to bring the two spatially orthogonal modes of the coil to resonance at the same frequency. The decoupling of the two modes is better than -35 dB. The tuned and matched coil is housed in a RF shielded enclosure.

Two spectrometers were set up for the circularly polarized NQR experiments described here. One is a standard, homebuilt low-frequency spectrometer controlled by a Chemagnetics pulse programmer and the other is a Tecmag NQRkit (reference to a particular product is for identification only; other products from other vendors may well be equally suitable for this application). To both, the following additions were made. The output of the high-power transmitter is split by a homebuilt high-power quadrature splitter (*16*) before going to the probe. This narrowband splitter is designed to handle the 3.5-kW output of the transmitter. The outputs are balanced to within 1 dB and the phase shift is within 2° of quadrature. For linearly polarized experiments, one of the quadrature splitter ports was terminated in 50 Ω, as was one of the inputs to the probe. Note that these additions require no modification of the spectrometer.

A special preamplifier setup (Fig. 7) is used to allow the simultaneous separate detection of both laboratory frame quadrature components of the circularly polarized RF signal with our standard single-channel receiver. The two outputs of the probe are connected to separate transmit/receive (T/R) switches and separately amplified by two preamplifiers chosen to have the same gain. (The input to one preamp was terminated in 50 Ω for linearly polarized detection.) The output of one preamp (PA) is attenuated by 3 dB and the other (PB) is split by a $0^\circ/180^\circ$ power splitter. The outputs of the splitter are fed to the inputs of a commercial SPDT GaAs FET switch. The output of the switch and the signal from PA are combined in a power combiner and sent to the receiver for further amplification, demodulation, and digitization. The polarity of the switch is inverted for alternating samples so that the total signal alternates between (PA + PB) and (PA − PB).

The signal is oversampled and in post-processing adjacent data points are combined appropriately to obtain either PA or PB. PA and PB can then be combined to increase the SNR and determine the sense of signal rotation in the laboratory frame. The two laboratory frame circularly polarized signals are obtained (in the rotating frame) from $\mathrm{PA} \pm \mathrm{PB}^*$, where PB^* denotes the complex conjugate of PB. Which of these gives the circularly polarized signal with the same sense of rotation as the applied circularly polarized field is determined by the sign of the phase shift of the quadrature splitter on the transmitter.

The NQR sample used was 2.5 kg of sodium nitrite. As a source of magnetoacoustic ringing, which could be used to test the system, it was found that a pair of locking pliers placed in the coil provided a convenient artifact signal, presumably from the chrome plating. All experiments were performed at room temperature on the ^{14}N ν_+ line at 4.64 MHz. The data in Figs. 4 and 5 were obtained in the small volume coil from the same two-pulse sequence by collecting data after both pulses. The data in Fig. 6 were obtained in the large volume coil with a one-pulse sequence. The pulse length for maximum signal with linearly polarized excitation/detection was 200 μs in the large volume coil and 150 μs in the small-volume coil. The pulse nutation angle was adjusted by varying the pulse duration; however the pulse areas are used here to correct for measurable pulse droop.

In Fig. 5, the predicted curves were obtained by numerical integration over the powder orientations. The SOPHE method (*17*) was used to generate 208 (θ, φ) pairs. These pairs were then optimized with the REPULSION method (*18*). Without the optimization step, numerical integration of Eq. [4] using $B_{\mathrm{eff}}^{\mathrm{r}} = \cos\theta$ and $B_{\mathrm{eff}}^{\mathrm{t}} = \mathbf{B}_{1\mathrm{L}}(\theta, \varphi)$ did not adequately reproduce the analytical results, Eq. [5], which was the case even when more than 7000 (θ, φ) pairs were used.

CONCLUSIONS

The use of circularly polarized RF fields for NQR excitation of a spin $I = 1$ powder results in a 1.72 times increase in the detected signal, similar to the $I = \frac{1}{2}$ NMR case. Unlike the NMR case, where the increased signal comes from improved detection of the precessing spins, the NQR signal gain arises

primarily from excitation and detection of a larger fraction of the spins in a powder sample. The use of a circularly polarized RF field improves the excitation field homogeneity for powder samples, reducing the pulse nutation angle necessary for maximum signal. This should prove advantageous in many multiple-pulse experiments. The NQR signal resulting from circularly polarized excitation is also circularly polarized, a feature that can be used to help differentiate it from artifacts such as magneto-acoustic and piezoelectric ringing that usually produce only linearly polarized signals.

ACKNOWLEDGMENTS

Our thanks to Professor G. Miller (University of Maryland) for construction of the large-volume birdcage coil used in these studies. This work has been sponsored in part by the U.S. Federal Aviation Administration, the Office of Special Technology (U.S. Department of Defense) and the U.S. Defense Advanced Research Projects Agency.

A paper on circular polarization ^{14}N NQR recently appeared (*19*), after the present paper was submitted for publication. We note that their results are also consistent with the theory presented here.

REFERENCES

1. T. P. Das and E. L. Hahn, "Nuclear Quadrupole Resonance Spectroscopy," Academic Press, New York (1958).
2. S. Vega, Influence of the Overhauser effect on ^{14}N PNQR T_1 measurements on a single crystal of parachloroaniline, *J. Chem. Phys.* **63,** 3769–3778 (1975).
3. S. Vega and A. Pines, Operator formalism for double quantum NMR, *J. Chem. Phys.* **66,** 5624–5644 (1977).
4. (a) M. L. Buess, A. N. Garroway, J. B. Miller, and J. P. Yesinowski, Explosives detection by ^{14}N pure NQR, *in* "Advances in Analysis and Detection of Explosives" (J. Yinon, Ed.), pp. 361–368, Kluwer, Dordrecht, Netherlands (1993); (b) A. N. Garroway, M. L. Buess, J. P. Yesinowski, J. B. Miller, and R. A. Krauss, Explosives detection by nuclear quadrupole resonance (NQR), *SPIE Proc.* **2276,** 139–148 (1994).
5. D. I. Hoult, C.-N. Chen, and V. J. Sank, Quadrature detection in the laboratory frame, *Magn. Reson. Med.* **1,** 339–353 (1984).
6. C.-N. Chen and D. I. Hoult, "Biomedical Magnetic Resonance Technology," Adam Hilger, New York (1989).
7. S. Vega, Theory of T_1 relaxation measurements in pure nuclear quadrupole resonance of spins $I = 1$, *J. Chem. Phys.* **61,** 1093–1100 (1974).
8. M. Bloom, E. L. Hahn, and B. Herzog, Free magnetic induction in nuclear quadrupole resonance, *Phys. Rev.* **97,** 1699–1709 (1955).
9. M.-Y. Liao and D. B. Zax, Analysis of signal-to-noise ratios for noise excitation of quadrupolar nuclear spins in zero field, *J. Phys. Chem.* **100,** 1483–1487 (1996).
10. M. J. Weber and E. L. Hahn, Selective spin excitation and relaxation in nuclear quadrupole resonance, *Phys. Rev.* **120,** 365–375 (1960).
11. T. Charpentier, Investigation of the effect of a rotating excitation in pure NQR spectroscopy of spin 3/2 nuclei, *in* "Abstracts of the 28th Congress Ampere" (M. E. Smith and J. H. Strange, Eds.), pp. 509–510, Univ. of Kent, Canterbury, UK (1996).
12. Ya. S. Greenberg, Application of superconducting quantum interference devices to nuclear magnetic resonance, *Rev. Mod. Phys*. **70,** 175–222 (1998).
13. C. E. Hayes, W. A. Edelstein, J. F. Schenck, O. M. Mueller, and M. Eash, An efficient, highly homogeneous radiofrequency coil for whole-body NMR imaging at 1.5 T, *J. Magn. Reson.* **63,** 622–628 (1985).
14. F. D. Doty, G. Entzminger, Jr., C. D. Hauck, and J. P. Staab, Practical aspects of birdcage coils, *J. Magn. Reson.* **138,** 144–154 (1999).
15. M. C. Leifer, Resonant modes of the birdcage coil, *J. Magn. Reson.* **124,** 51–60 (1997).
16. J. B. Hagen, "Radio-frequency Electronics," Cambridge Univ. Press, Cambridge, UK (1996).
17. D. Wang and G. R. Hanson, A new method for simulating randomly oriented powder spectra in magnetic resonance: The Sydney opera house (SOPHE) method, *J. Magn. Reson. A* **117,** 1–8 (1995).
18. M. Bak and N. C. Nielsen, REPULSION, a novel approach to efficient powder averaging in solid-state NMR, *J. Magn. Reson.* **125,** 132–139 (1997).
19. Y. K. Lee, H. Robert, and D. K. Lathrop, Circular polarization excitation and detection in N-14 NQR, *J. Magn. Reson.* **148,** 355–362 (2001).